Electronic Supplementary Material (ESI) for CrystEngComm.

Supplementary Information

Designing 3D nanoporous network via self-assembly of WO_3 nanorods for improved electrocapacitive performance

Akshay V. Salkar[a], Amarja P. Naik[a], Vrushali S. Joshi[a], Santosh K. Haram[b] and Pranay P. Morajkar[*,a]*

[a] Department of Chemistry, Goa University, Taleigao Plateau, 403206, Goa, India.

[b] Department of Chemistry, Savitribai Phule Pune University, Pune 411007, Maharashtra, India.

* Email: pranay@unigoa.ac.in

Content

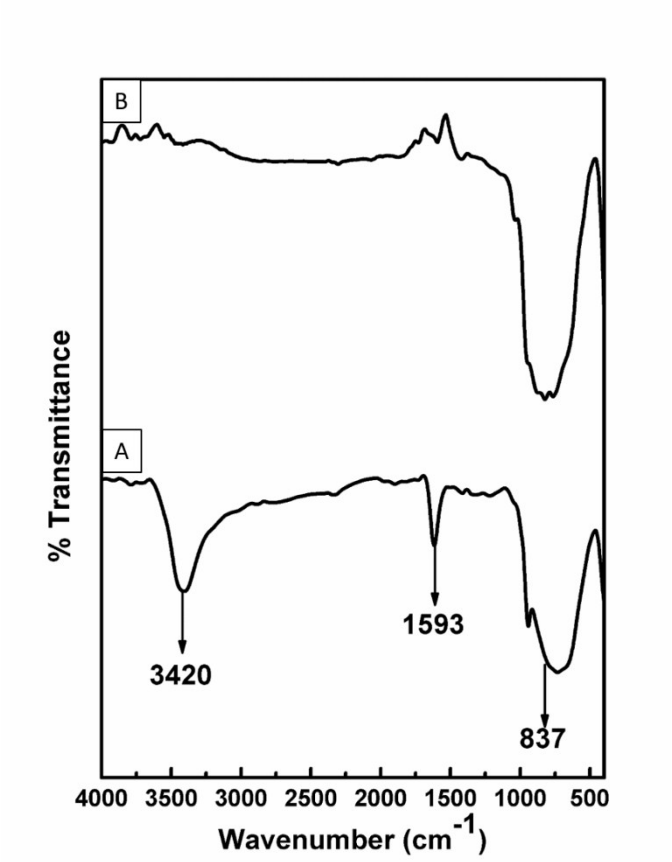

Figure S1. IR spectra of (A) Tungstic acid gel dried at 150°C and (B) Pristine WO_3 after calcination at 550°C

The IR spectra of tungstic acid gel dried at 150°C shows peak at 3420 cm^{-1} which corresponds to the stretching mode of OH group, a peak at 1593 cm^{-1} corresponding to bending vibration for adsorbed water and broad absorption peaks from 1000-600 cm^{-1} characteristic of the different O-W-O stretching vibrations in the WO_3 crystal lattice. In the IR spectra of pristine WO_3 the OH stretching and bending modes are significantly lowered while the O-W-O stretching vibrations remain visible.[1]

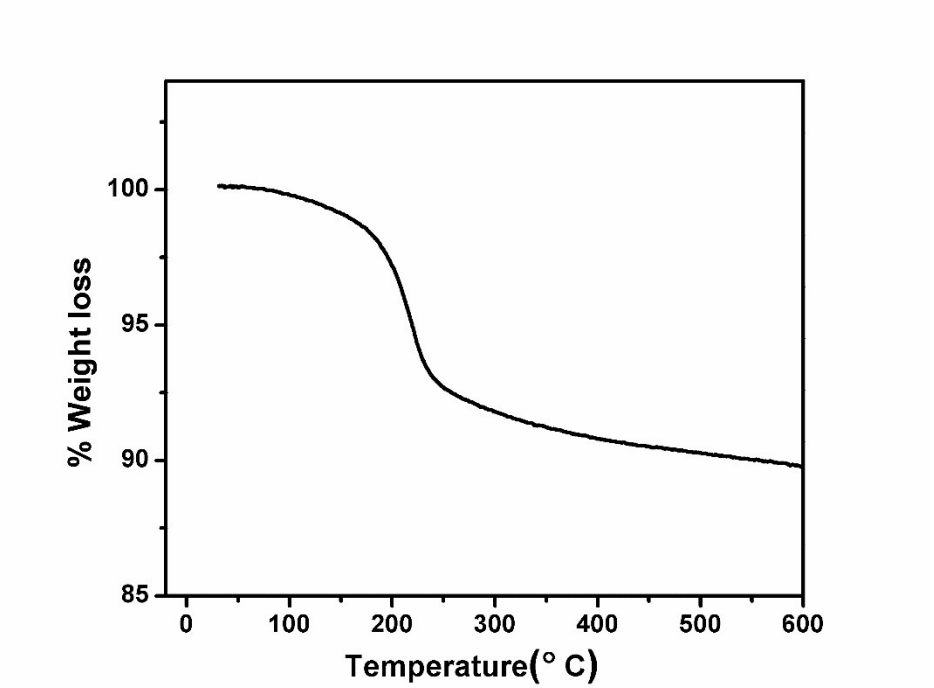

Figure S2. TG curve of tungstic acid gel dried at 150°C

The above TG curve represents the as synthesized tungstic acid gel without urea. An overall weight loss of 10% is observed which can be accounted for the loss of water molecules from tungstic acid in order to form tungsten trioxide.

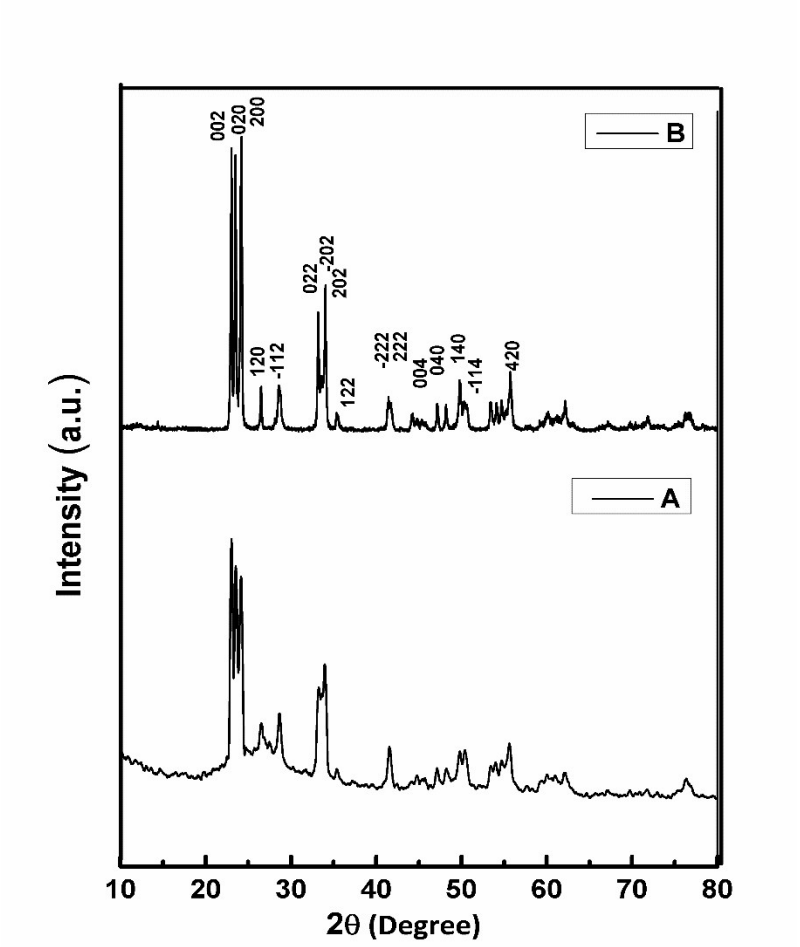

Figure S3. XRD pattern of synthesized (A) WO_3 nanostructures after 4h and (B) WO_3 nanostructures after 8h calcination at 550°C.

Figure S3 confirms the formation monoclinic phase of nanostructured WO_3 at calcination times of 4h (Figure S3 A) and 8h (Figure S3 B) in accordance with the JCPDS card number 43-1035.

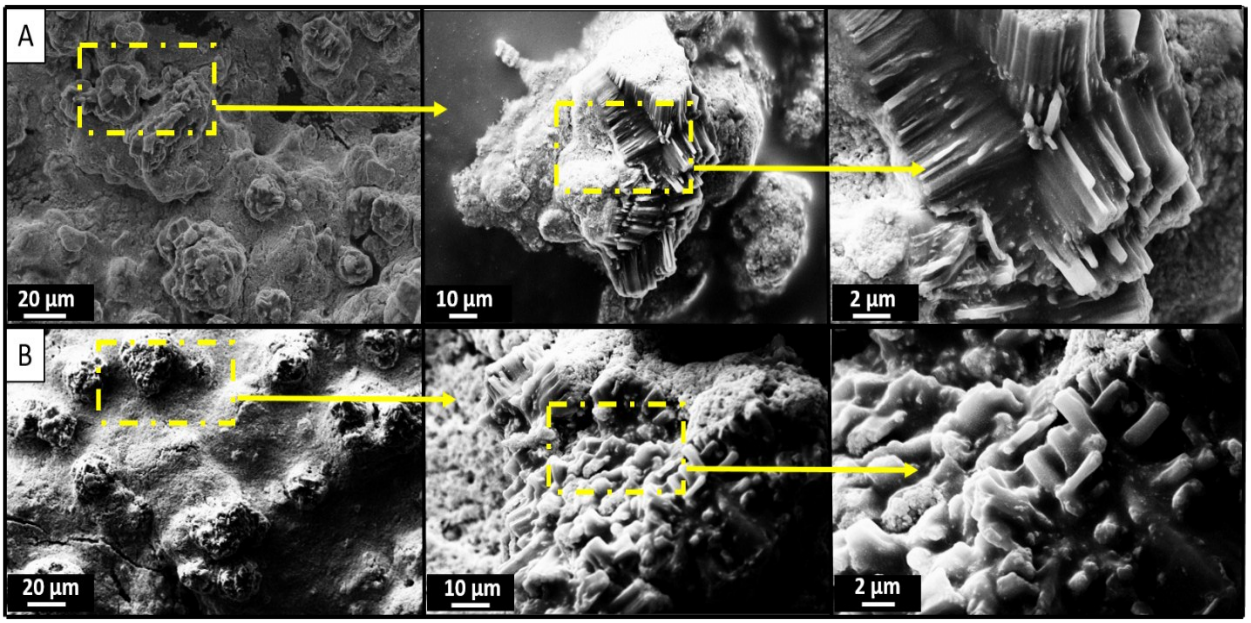

Figure S4. SEM images showing sintering effect and loss of porous nanostructured morphology of the synthesized W_4 and W_5 samples at longer calcination time of A) 6h and B) 8h respectively.

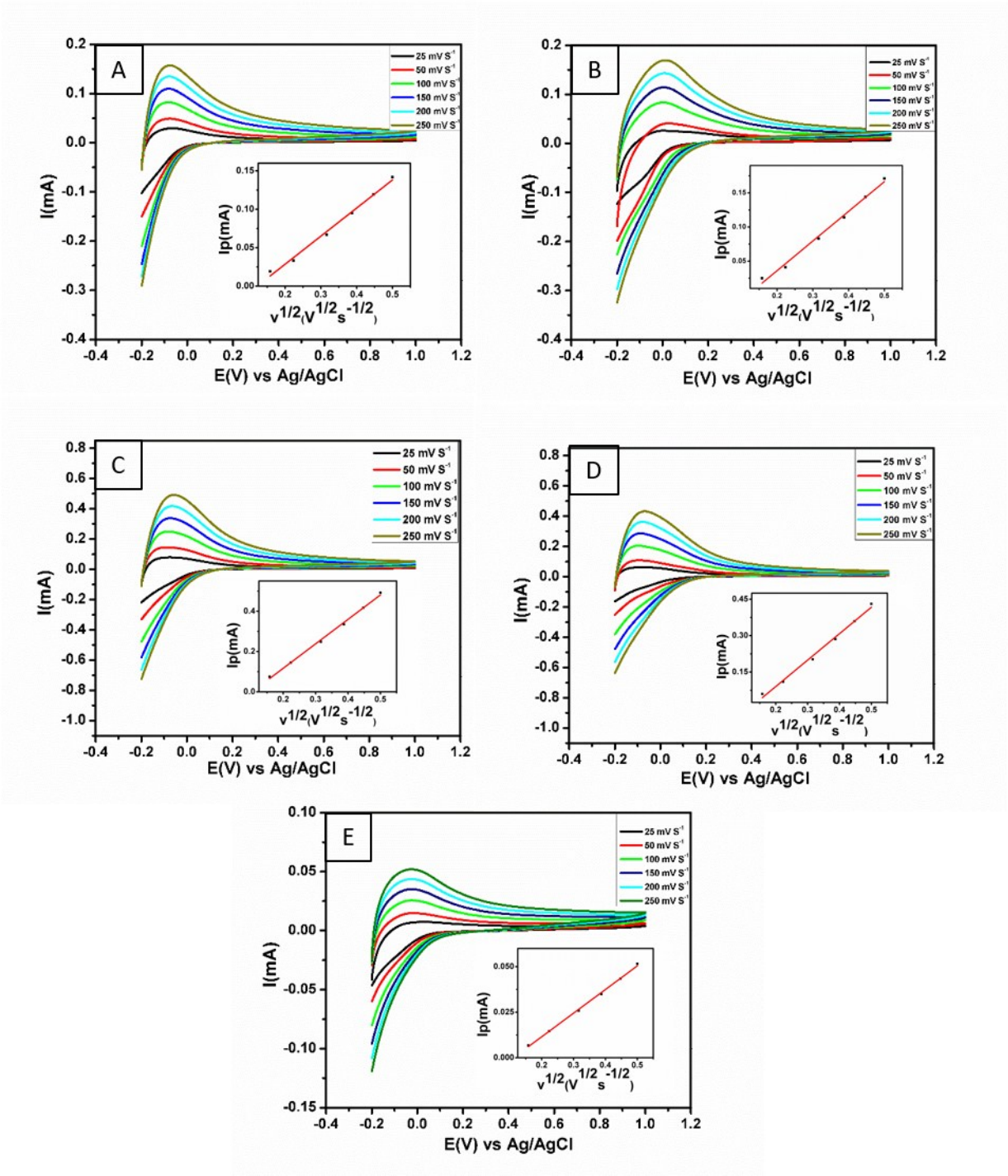

Figure S5. CV curves of (A) W_1=WO_3 nanoparticles (B) W_2=WO_3 nanorods (C) W_3=WO_3 nanoporous network after 6h calcination (D) W_4=WO_3 nanoporous network after 8h calcination (E) W_6=WO_3 sheets. The insets give the chart for current Ip vs square root of scan speed $v^{1/2}$.

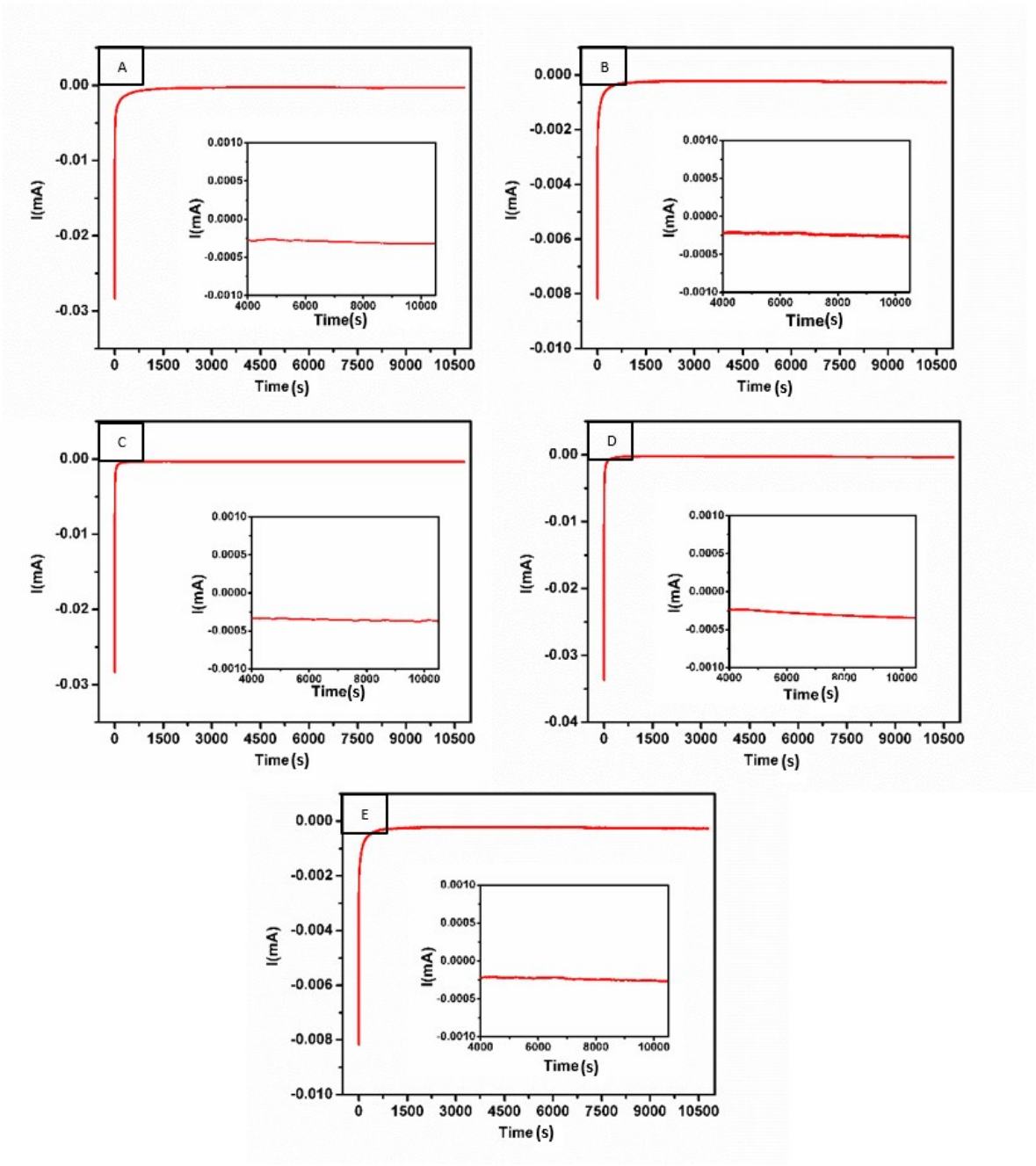

Figure S6. Film stability investigated using chronoamperometry for WO_3 (A) Nanoparticles (B) Nanorods (C) Nanoporous network calcined for 6h (D) Nanoporous network calcined for 8h (E) Nanosheets.

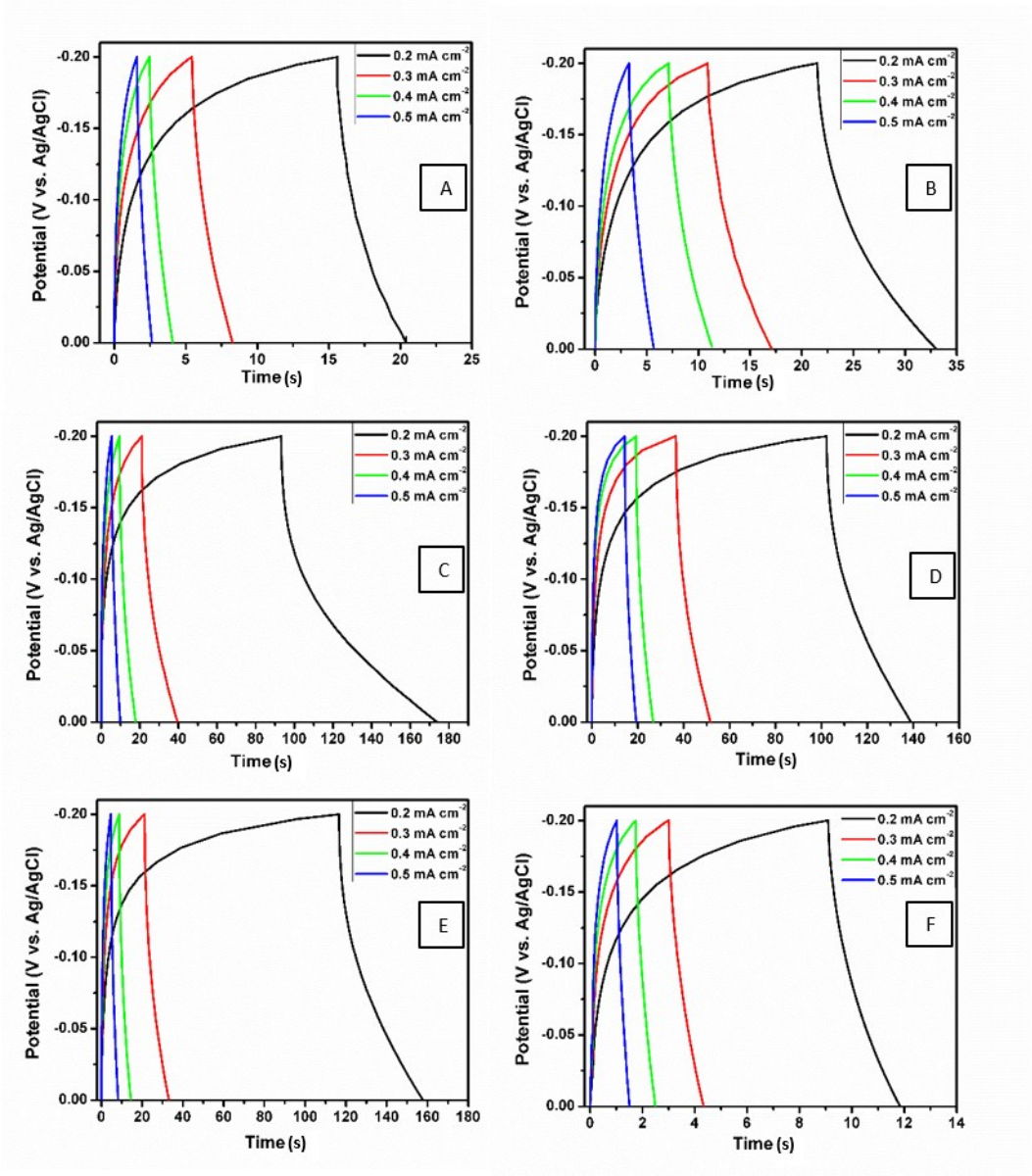

Figure S7. Galvanostatic charge discharge curves at variable current densities recorded on 3mm dia. modified glassy carbon electrode for WO_3 (A) Nanoparticles (B) Nanorods (C) Nanoporous network calcined for 4h (D) Nanoporous network for 6h (E) Nanoporous network for 8h (F) Nanosheets.

Table S1. Comparison of capacitance values obtained from galvanostatic charge discharge.

	*Capacitance (F/g)			
Current Density (mA/g) ⟶	0.02 mA/g	0.03 mA/g	0.04 mA/g	0.05 mA/g
W_1	4.7	4.2	0.3	0.3
W_2	11.3	9.3	0.9	0.6
W_3	78.5	28.3	1.8	0.9
W_4	40.9	22.4	1.4	1.4
W_5	36.8	18.5	1.1	0.8
W_6	2.8	2.0	0.2	0.1
*Values are estimated from charge discharge curve recorded on a 3 mm glassy carbon modified electrodes.				